

REPORT DOCUMENTATION PAGE

Form Approved
OMB No. 0704-0188

The public reporting burden for this collection of information is estimated to average 1 hour per response, including the time for reviewing instructions, searching existing data sources, gathering and maintaining the data needed, and completing and reviewing the collection of information. Send comments regarding this burden estimate or any other aspect of this collection of information, including suggestions for reducing the burden, to Department of Defense, Washington Headquarters Services, Directorate for Information Operations and Reports (0704-0188), 1215 Jefferson Davis Highway, Suite 1204, Arlington, VA 22202-4302. Respondents should be aware that notwithstanding any other provision of law, no person shall be subject to any penalty for failing to comply with a collection of information if it does not display a currently valid OMB control number.

PLEASE DO NOT RETURN YOUR FORM TO THE ABOVE ADDRESS.

1. REPORT DATE (DD-MM-YYYY) 12/21/2015		2. REPORT TYPE Final Technical Report		3. DATES COVERED (From - To) -1 Mar 2011 to 30 Sept 2015	
4. TITLE AND SUBTITLE Spontaneous energy concentration in energetic molecules, interfaces and composites: response to ultrasound and THz radiation				5a. CONTRACT NUMBER	
				5b. GRANT NUMBER N00014-11-1-0418	
				5c. PROGRAM ELEMENT NUMBER	
6. AUTHOR(S) Dana D. Dlott Kenneth S. Suslick				5d. PROJECT NUMBER	
				5e. TASK NUMBER	
				5f. WORK UNIT NUMBER	
7. PERFORMING ORGANIZATION NAME(S) AND ADDRESS(ES) The board of trustees of the university of Illinois at Urbana-Champaign Grants and Contracts Office 1901 South First St. Suite A Champaign, IL 61820-7406				8. PERFORMING ORGANIZATION REPORT NUMBER	
9. SPONSORING/MONITORING AGENCY NAME(S) AND ADDRESS(ES) Michael Schlesinger ONR 301 and Joong Kim ONRA 30 Office of Naval Research 875 North Randolph St. Arlington, VA 22203-1995				10. SPONSOR/MONITOR'S ACRONYM(S) ONR	
				11. SPONSOR/MONITOR'S REPORT NUMBER(S)	
12. DISTRIBUTION/AVAILABILITY STATEMENT Approved for Public Release; Distribution is Unlimited					
13. SUPPLEMENTARY NOTES					
14. ABSTRACT The effects of weak energies, THz and ultrasound, on energetic materials, was studied experimentally using laser vibrational spectroscopies and time-resolved thermal imaging microscopy.					
15. SUBJECT TERMS Ultrasound, THz radiation, energetic materials, hot spots, energy concentration					
16. SECURITY CLASSIFICATION OF:			17. LIMITATION OF ABSTRACT	18. NUMBER OF PAGES	19a. NAME OF RESPONSIBLE PERSON
a. REPORT	b. ABSTRACT	c. THIS PAGE			Dana D. Dlott
UU	UU	UU	UU	15	19b. TELEPHONE NUMBER (Include area code) 217-333-3574

20160112049

Award Information

Award Number	N00014-11-1-0418
Title of Research	Spontaneous energy concentration in energetic molecules, interfaces and composites: response to ultrasound and THz radiation
Principal Investigators	Dana D. Diott and Kenneth S. Suslick
Organization	University of Illinois at Urbana-Champaign
Performance period	01 Mar 2011 to 30 Sept 2015

Technical Section

Technical Objectives

This project involves fundamental research to investigate the detailed effects of THz and ultrasound, so called “weak energies”, on energetic materials (EM). The focus is on mechanisms that produce spontaneous energy concentration. The relevant Navy mission is the potential use of weak energies to modify the initiation process to defeat EM, especially in the form of IEDs, by making detonation impossible. This might be accomplished in two ways: (1) using weak energies to cause an explosive to burn gradually, avoiding deflagration-to-detonation transitions (DDT), by creating a number of hot spots too small to sustain explosive growth,⁵ or (2) rendering the EM insensitive to impact initiation by consuming a significant fraction of the explosive content or by consuming defect sites to suppress hot spot formation, so that the detonator becomes ineffective. Another closely-related application is the use of weak energies to stimulate unique responses from EM to enhance technologies used for remote detection.

Weak energies will have effects on EM only when mechanisms exist to concentrate the weak energy into localized spatial regions, to create hot spots. In this project, we focus on energy concentration mechanisms at various levels of length scales and complexity. Working down in size scale, these include the composite structures associated with practical EM such as plastic-bonded explosives (PBX), or plastic-bonded explosive simulants (PBS), the individual grains of EM with and without binders, the interfaces between EM and binders, and individual molecules that comprise an EM.

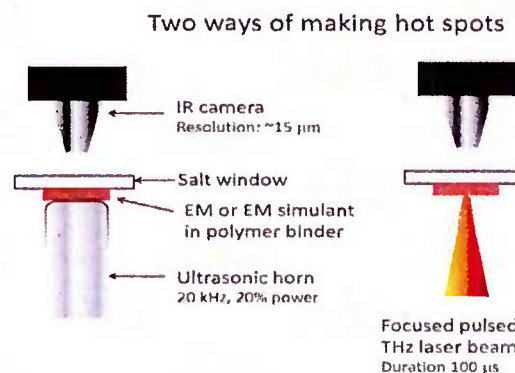


Figure 1. Two ways of making hot spots that can be detected by an IR microscope: ultrasound and focused pulsed THz radiation. The microscope allows us to image and to time resolve the hot spots.

Technical Approach

In this project, we developed new experimental techniques and used them to study the concentration of weak energies in four ways.

1. At the level of individual molecules, we looked at molecules with nitro functional groups, such as nitrobenzene and nitromethane, in the liquid state. The nitro groups were excited using ultrashort bursts of THz radiation, and the energy flow in and out of the nitro groups was monitored using Raman spectroscopy. The combination of Stokes and anti-Stokes Raman provides a quantitative measure of the energy in different vibrational states of the molecules, so energy flow and concentration could be monitored in real time. The combination of THz excitation and Raman probing created a new method in vibrational spectroscopy that was three dimensional.⁶ The three dimensions were the vibrational frequency being excited, the vibrational frequency being probed and the time between excitation and probing.
2. At the level of material interfaces, we chemically bonded nitro-containing molecules such as nitrobenzene thiol ($\text{HS-C}_6\text{H}_4\text{-NO}_2$; NBT) to metal surfaces such as Au. A visible femtosecond light pulse was used to flash-heat the Au surface.⁷⁻¹² After about one picosecond, this energy was converted into lattice excitations that oscillated at THz frequencies.⁷ As this excess energy was transferred to the colder bonded molecules, we probed their nitro groups using ultrafast vibrational sum-frequency generation spectroscopy (SFG),^{13,14} which is a nonlinear coherent spectroscopy that is particularly useful for studying fast processes at interfaces.
3. At the level of bulk materials, we developed a high-speed thermal imaging microscope apparatus.^{15,16} Looking through this microscope at crystals of EM, such as RDX or HMX and HMX-containing plastic-bonded explosives (PBX), we irradiated the crystals with tunable THz radiation, and we looked to see how the heating caused by this radiation became localized in the EM.^{15,16}
4. At the level of bulk composite materials, we used the high-speed thermal imaging microscope to look at EM and EM simulants consisting of various selected combinations of crystals and polymer binders, while the samples were irradiated by 20 kHz ultrasound.¹⁵ The ultrasound could gently heat these materials at lower intensities, but at higher intensities rapid heating could occur that would cause the EM to explode.¹⁷

Progress Statement Summary

We successfully completed studies of energy concentration in molecules with nitro groups using ultrafast three-dimensional vibrational spectroscopy. We completed studies of energy concentration of nitro-group containing molecules at interfaces using ultrafast sum-frequency spectroscopy. We developed a unique thermal imaging microscope apparatus and used it to study how THz radiation became concentrated inside EM crystals, and how ultrasound energy became concentrated in composite materials that contained EM.

Technical Section

1. Energy concentration by nitro groups

Nitro groups have a number of characteristic THz transitions such as symmetric (42 THz) and asymmetric stretching (48 THz), wobbling (14.4 THz) and scissoring (20 THz).^{4,6} Using our THz-Raman apparatus, where an intense THz pulse is allowed to excite nitro groups and a combination of Stokes and anti-Stokes Raman probing reveals how the energy is redistributed throughout the molecule,^{4,6,18} we could track the energy flow and concentration in real time. We have been focusing on liquid nitromethane and nitrobenzene due to their interesting nitro vibrational behavior. By scanning the frequency of the ~1 ps duration THz pulses and detecting the results ~1 ps after the pulse, we can see the initial phase of vibrational energy redistribution and concentration. Some data on liquid nitromethane at room temperature are shown in Fig. 2.⁶

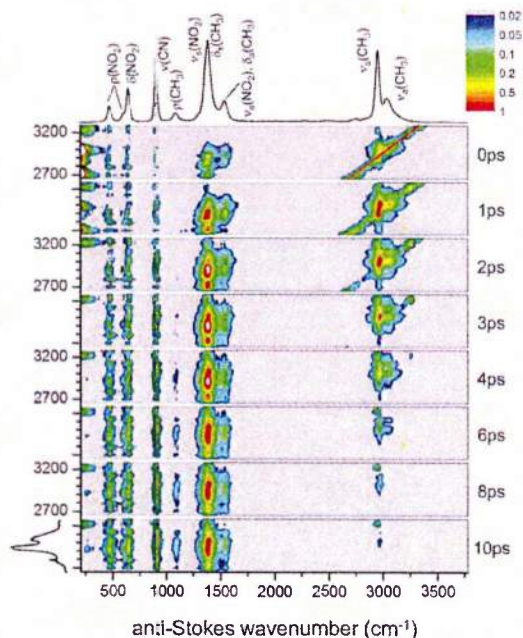


Figure 2. Three dimensional vibrational spectrum of nitromethane liquid. The nitro excitations are in the 1300-1600 cm^{-1} range and near 480 cm^{-1} . Energy was input in the 81-93 THz range.

Our most interesting results were obtained using nitrobenzene and substituted nitrobenzenes.^{3,4} We think of nitrobenzene as consisting of a nitro group bonded to a phenyl ring. The THz pump pulse energy was varied in the 81-93 THz region, where CH-stretch and NO_2 stretch $\nu = 2$ overtones can be excited. The ν_{CC} vibration is a ring stretch and the ν_{NO} vibrations are nitro vibrations. With the lower THz pulses, there was a lot of vibrational energy in the phenyl group. (The ν_{CC} stretch is used as a marker of phenyl excitation). In addition, energy also appeared in the nitro group, indicating efficient phenyl-to-nitro energy transfer. With the higher THz pulses, the energy was deposited on the nitro groups, and very little of the phenyl excitation was created. This type of energy localization on a substituent has been seen so far only in nitro compounds. A cartoon summary of this process, which indicates that nitrobenzene can support one-way vibrational energy transfer (a “vibrational energy diode”) is shown at the top of Fig. 3.

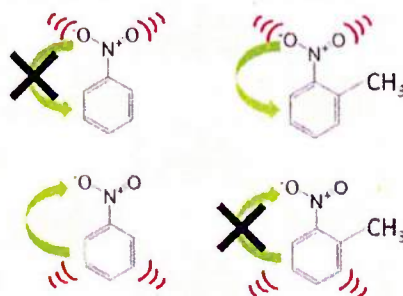


Figure 3. Cartoon summary of results using three-dimensional vibrational spectroscopy to study energy localization in nitrobenzenes. (left) In nitrobenzene, energy flows from phenyl-to-nitro but does not flow from nitro-to-phenyl. (right) In nitrotoluene, the methyl group reverses the direction of energy flow.^{3,4}

We completed our studies of energy concentration at molecular nitro groups, using three-dimensional vibrational spectroscopy.^{3,4,6} One example of that method is shown in Fig. 2. The nitro energy

was produced by vibrationally exciting the nitro groups of nitrobenzene in the mid-infrared (high THz). As mentioned above, we discovered that the nitrobenzene molecule was a kind of vibrational energy diode, where energy transfer between nitro and phenyl was unidirectional.⁴ In the next study, we looked at the effects of substituting other groups on these molecules. This is the realization of one of the ideas of Dan Prono, who wanted to understand how something such as the methyl group in trinitrotoluene (TNT) affected energy concentration. As illustrated in the cartoon in Fig. 3, we found that adding a methyl group (i.e. nitrotoluene) reversed the direction of the vibrational diode.³ Energy with the methyl group now flowed from nitro-to-phenyl but not vice versa. We tried some other substituents such as fluoro, but the effects were not as dramatic.³ Brandt Pein, who led this project, has obtained his Ph.D. and is now a postdoc at MIT with Prof. Keith Nelson.

2. Interfacial nitro group energy

An experimental apparatus was developed to study energy flow from a metal surface into a monolayer of molecules containing nitro groups. We studied nitrobenzene thiol (NBT) molecules bonded to Au or nitrobenzoic acid (NBA) molecules bonded to Al surfaces, in the form of self-assembled monolayers (SAMs),^{9-11,19} using a recently-developed advanced method of SFG spectroscopy.¹³ Energies were input into the molecules by flash-heating the Au surface, producing THz-frequency lattice vibrations, or by driving laser-generated GPa shocks into an Au or Al surface that passed over a monolayer of the molecules. The experimental apparatus and sample arrangements are depicted in Fig. 4.

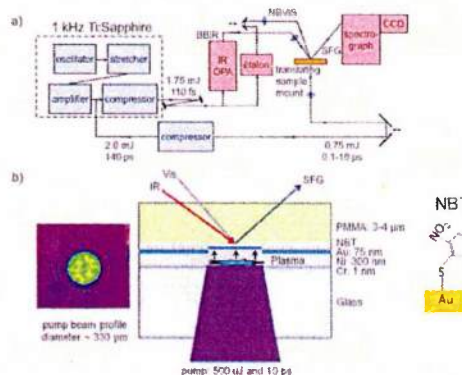


Figure 4. (a) Schematic of laser apparatus. (b) Image of top-hat laser drive beam, layout of a single element of the target array, and structure of nitrobenzenethiol (NBT) monolayer.

Figure 5 shows shock compression data obtained from the NO_2 symmetric stretching transition near 1335 cm^{-1} . We made two types of measurements. First we studied the static high pressure response of a monolayer of NBT on Au in a SiC anvil cell. It is difficult to obtain information about the vibrational spectra of nitro groups in a monolayer, due to the small number of molecules. We overcame this difficulty by fabricating a tiny photonic chip that amplified the Raman signal by a factor of 10^6 .^{20,21} The pressure-dependent frequency blueshift of the symmetric nitro stretch vibration of NBT in a SiC anvil cell is shown in Fig. 5a. Second we monitored the same nitro groups in a shock experiment where a GPa laser-driven shock was propagated through an NBT or NBA monolayer on Au or Al planar substrates using SFG, as shown in Fig. 5b.⁹ Time $t = 0$ was when the shock drive laser pulse arrived; the shock reached the NBA monolayer about 45 ps later, which was the time for shock formation and propagation through 375 nm of Al. When the shock arrived, it caused a sudden ($t_r = 6$ ps) loss of SFG intensity and a peak blueshift of 3 cm^{-1} . Based on the static high pressure results, the shock was 1.5 GPa.

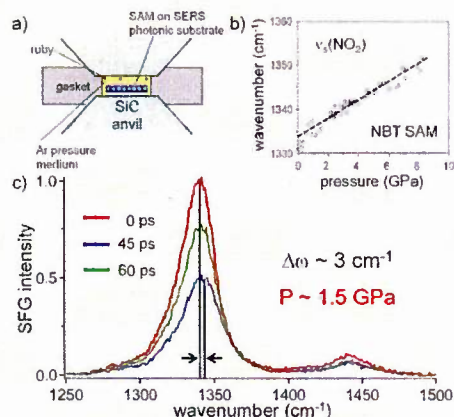


Figure 5. (a) SiC high pressure cell with a surface-enhanced Raman scattering (SERS) photonic substrate used to amplify NBT monolayer Raman signals. (b) Calibrating the $\nu_s(\text{NO}_2)$ frequency shift to a known pressure using hydrostatic measurements. (c) Spectra of the shock loaded NBT SAM. When shock arrived at 45 ps, the blueshift was 3 cm⁻¹, indicating a pressure of 1.5 GPa.

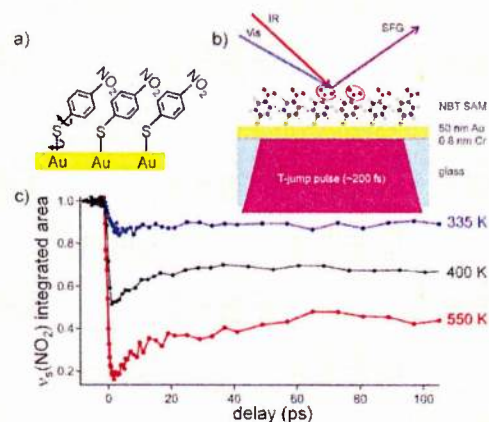


Figure 6. (a) Excitation of 4-nitrobenzenethiol (NBT) rotational modes by flash-heating the underlying Au substrate. (b) Flash-heating setup with temperature jump (T-jump) pulse and SFG probe. (c) Time-dependent response from the symmetric nitro $\nu_s(\text{NO}_2)$ mode of NBT at various indicated temperatures, which were ascertained from thermoreflectance of the Au surface.^{1,2}

Flash-heating experiments are described in Fig. 6. To characterize the flash-heating, we first measured the temperature-dependence of Au reflectivity change at 600 nm, $\Delta R/R$, in an oven with a thermocouple, which gave an optical thermometer equation for Au,

$$\Delta R/R = -1.33 \times 10^{-4} \Delta T.^7$$

In Fig. 6, NBT molecules on Au were subjected to the large-amplitude temperature jumps (up to $\Delta T = 300\text{K}$)¹² indicated in the Figure. Time zero marked the flash-heating pulse arrival at the substrate. The SFG intensity dynamics after T-jump had an overshoot-decay-plateau structure (Fig. 6c), where the overshoot resulted from direct excitation of nitro groups by Au hot electrons generated during laser flash-heating. After the hot electron effects decayed away, a plateau was reached that indicated the SAM was in equilibrium with the THz-frequency phonons in the flash-heated Au layer.¹ SFG intensity within the plateau regime decreased with increasing monolayer disorder, which resulted from thermal excitation of SAM rotational modes (Fig. 6a).²²

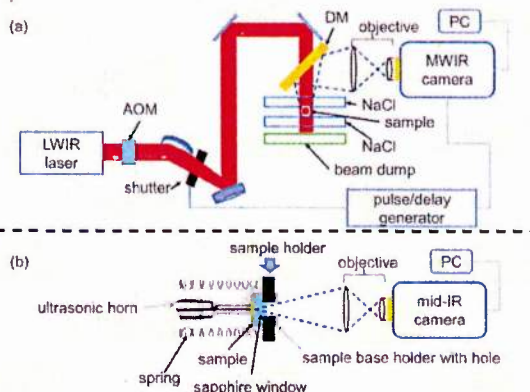


Figure 7. (a) Schematic of thermal imaging microscope used to study hot spots created by long-wavelength infrared (LWIR) laser beams. Key: MWIR = mid-wavelength IR, DM = dichroic mirror, AOM = acoustooptic modulator. (b) Schematic for MWIR microscope to study hot spots created by ultrasound.

3. THz irradiation of explosives

The THz and ultrasound experiments used a novel fast thermal imaging microscope set up depicted in Fig. 7. This instrument was described in detail in a recent paper in the Review of Scientific Instruments.¹⁵ For the THz experiments, we used a long-wavelength infrared laser (LWIR) that was tunable near 30 THz.

The conventional wisdom would be that EM crystals irradiated by a THz laser would be heated most strongly when the radiation was tuned into strongly-absorbing transitions, but we made the surprising finding that that was not the case.¹⁶ Some representative data are shown in Fig. 8. The hot spots created in the RDX crystals are easily seen, and those hot spots were most prominent when the THz radiation was weakly-absorbing. An explanation for this unexpected result is shown in Fig. 9. The oblique planes of the RDX crystals act like THz lenses, creating hot spots at oblique junctions of crystal planes. But the hot spots cannot be created in this manner if the THz radiation does not penetrate into the crystals, so it was the weakly-absorbing, more-penetrating radiation that created the hot spots. This study provides needed insights into the wavelengths needed to produce energy localization in EM by THz radiation.

4. Ultrasound irradiation of energetic materials and simulants

In these experiments, we looked at RDX, an explosive, and sucrose, an EM simulant, in a polymer matrix, with the intent of understanding the effects of ultrasound on practical EM that

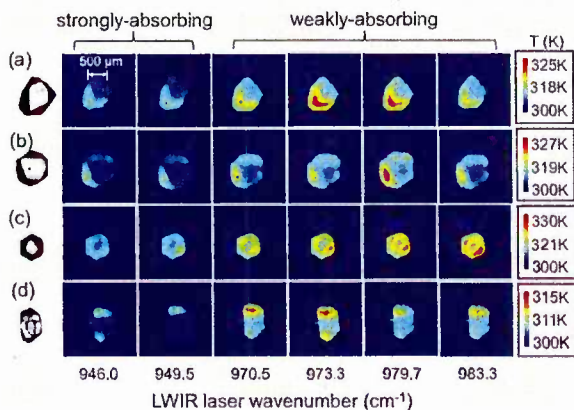


Figure 8. (a)-(d) Thermal images of RDX crystals irradiated for 450 ms by 3.5W LWIR pulses at the indicated wavenumbers. To the left of each row is an optical micrograph of each RDX crystal. Hot spots were associated with the oblique planes of the RDX crystals and were much more prominent with weakly-absorbed LWIR irradiation, than with the strongly-absorbing LWIR.

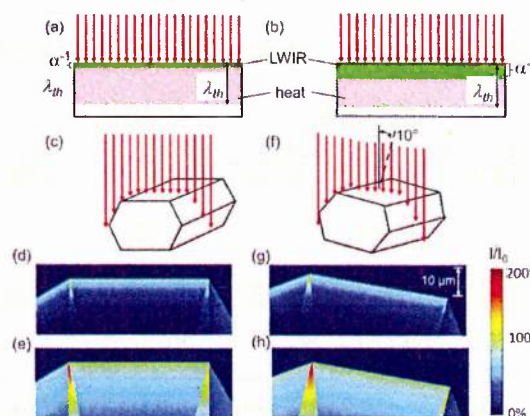


Figure 9. Models for LWIR irradiation of RDX slabs. (a) Strongly-absorbed and (b) weakly-absorbed regimes. During the 450 ms duration LWIR pulses, the RDX slabs were heated the same amount and to the same depth (λ_{th}) in both regimes, but LWIR penetrated more deeply into RDX in the weakly-absorbed regime. Models for LWIR refraction by a slab (c) with a plane normal to the LWIR beam, or (f) tilted 10° off the beam axis, both with oblique planes at 150° and 120° . In the strongly-absorbed regime, the absorption depth $\alpha^{-1} = 5 \mu\text{m}$. In the weakly-absorbed regime $\alpha^{-1} = 25 \mu\text{m}$. (d) Computed LWIR intensity inside RDX in the strongly-absorbed regime. (e) LWIR intensity in the weakly-absorbed regime. (f) LWIR intensity inside tilted RDX in the strongly-absorbed regime. (g) LWIR intensity in the tilted RDX in the weakly-absorbed regime. The LWIR intensity is concentrated where the flat and oblique planes meet, and the concentration effect is greater in the weakly-absorbed regime.

often consist of explosive ingredients and binders.^{15,17} For one example shown in Fig. 10, the EM was RDX in a polyurethane (estane) binder. In order to convert thermal images into temperatures, we needed to know the emissivities of these two materials in the mid-wave infrared (MWIR), so we performed static heating experiments and used analytic continuations of the data to temperatures above decomposition of the EM under static heating.¹⁵ Figure 10 is an example of the calibration method.

Figure 11 shows a few sucrose crystals embedded in silicone rubber under ultrasound. Not much heating, but the heat appeared at the polymer-crystal interfaces. This observation led to a major discovery. We realized that ultrasonic heating could be controlled by controlling the adhesion at disparate interfaces.

We next prepared samples where selected crystals were coated with a low-adhesion layer, either the slippery fluid polymer PEG or Teflon powder. Immediately we obtained stunning results. The coated crystals were heated at vastly greater rates. We could precisely control the localization of ultrasound energies, as illustrated in Fig. 12. {You, 2014 #3699}

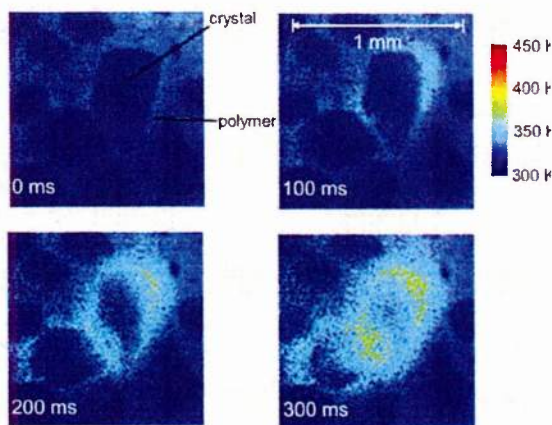


Figure 11. Thermal images of a few sucrose crystals embedded in silicone rubber irradiated by ultrasound for 300 ms. Not much heating, but the heat appears at the interfaces.

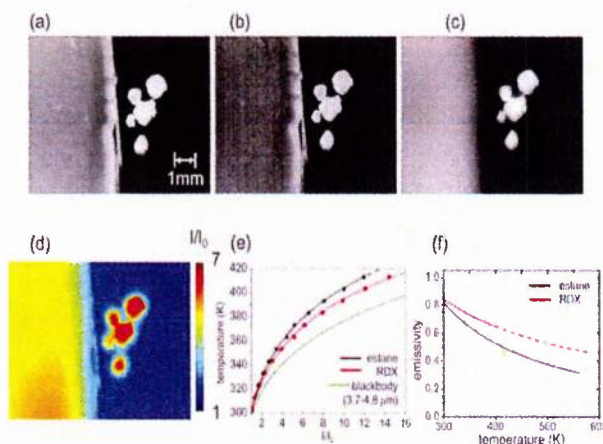


Figure 10. (a)-(c) Thermal micrograph of a few RDX crystals next to a slab of polyurethane (estane) at different temperatures. (d) False color thermal image. (e) Thermal emission intensity ratio, relative to ambient temperature for RDX and estane compared to a theoretical blackbody. (f) Measured temperature-dependent emissivities for estane and RDX. The dashed line is an analytic continuation for RDX above the temperature where it gradually decomposes.

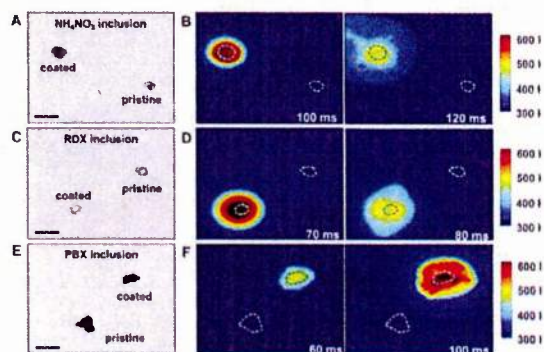


Figure 12. Ultrasound experiments on a polymer slab with two embedded crystals or crystalline composites. One crystal had a slippery surface coating and the other did not. The coated ammonium nitrate, RDX and PBX-9407 all got hot and exploded. The uncoated ones did not. Frames were obtained every 10 ms. The explosions happened faster than the interframe intervals (discussed further in Fig. 15).

The thermal imaging camera we used in these studies had an interframe interval of 10 ms. When an explosive crystal is irradiated with ultrasound, as in Fig. 12, the crystal heats up for several frames, corresponding to perhaps 50-100 ms. The explosive event is abrupt, and it always occurs in the interval between frames, so with this camera we see a crystal gradually heating for a few frames and then we see a crystal already exploded. The frame rate of the camera is limited by the physics of the detector material (Hg CdTe) and the readout time for the large number of pixels (328K). To overcome this limitation, we purchased a faster thermal imaging detector. In contrast to the frame camera, which is rectangular 640 x 512 with tiny 15 x 15 μm^2 pixels, and which can take one frame every 10 ms, the new camera is a linear array 32 x 1 with a digitizer that will let us read out data from all the pixels at 4 MHz for 32 ms. This fast linear array was a development plan of the manufacturer, Infrared Systems Development Corp., that was sponsored by the French government. We believe the French also wish to use this fast linear array for high-speed studies of energetic materials. As usual, the development was slower than originally proposed, so we asked for and received a 6 month unfunded extension of the grant. We took delivery of this new camera and we have obtained one interesting preliminary result. We used the frame camera to get snapshots of an HMX crystal in a silicone rubber polymer matrix being irradiated by ultrasound, and simultaneously used the linear camera to get a thermal history, with something like 2 μs time resolution, along one specified line running through the RDX crystal. The combination of the two cameras minimizes the drawbacks of each individual camera. The experimental set up for imaging ultrasound-irradiated samples with both cameras is shown in Fig. 13.

We have obtained some preliminary results with this new apparatus, as shown in Figs. 14 and 15. The sample was 0.5 mm HMX in silicone rubber polymer binder with a slippery PEG coating. As shown in Fig. 14, the HMX was heated rapidly by ultrasound, and somewhere between 30 and 40 ms it exploded. Now Fig. 15 shows the results from the fast linear array, which was

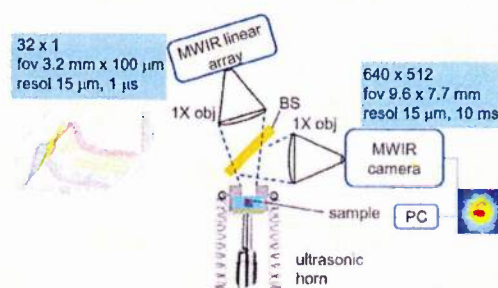


Figure 13. Thermal imaging microscopy apparatus that combines a 10 ms/frame mid-wavelength IR (MWIR) camera with a fast linear detector with 0.25 μm frame rate and a long record length.

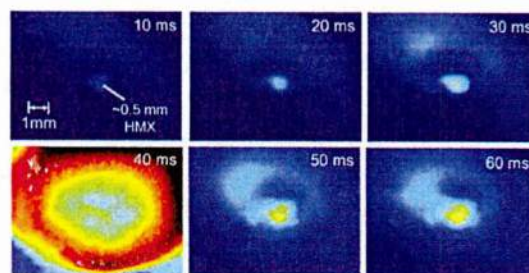


Figure 14. Thermal imaging microscopy movie of a 0.5 mm HMX crystal embedded in PDMS polymer, irradiated by ultrasound. The crystal exploded between 30 and 40 ms.

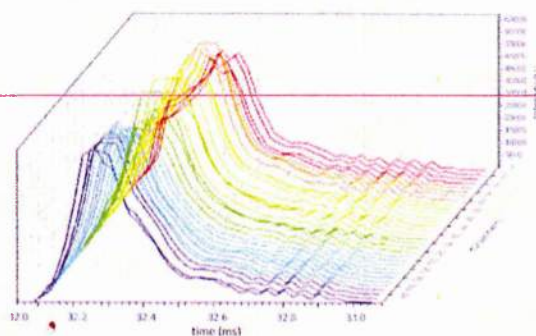


Figure 15. Output of the fast linear IR array obtained at the same time as Fig. 14. The HMX crystal was located between channels 25 and 32. It started to explode at 32.1 ms. The propagation of the explosion to more distant regions (channels 1-24) can be seen as the delayed rise times of those transients. Time resolution is 0.25 μs .

oriented so the HMX crystal was located between channels 25 and 32 (the blue range in Fig. 15). Now we can see that the HMX crystal started to explode at about 32.1 ms and that the explosion lasted about 0.4 ms. We can also see the explosion propagate, as seen by the delayed rises of the data transients in the lower-number channels (e.g. 2-8) in Fig. 15.

5. Technical section summary

We developed and utilized new methods to understand how THz and ultrasound weak energies are deposited and localized in energetic materials. Fundamental studies were performed to understand the detailed molecular dynamics that ensued when nitro-containing molecules were irradiated with THz radiation or GPa shocks. The effects of THz and ultrasound on EM crystals and composites were studied using advanced techniques in time-resolved thermal imaging microscopy. Two notable observations related to the mission of using THz or ultrasound to inactivate or detect IEDs were as follows: (1) THz radiation produced notable hot spots in EM solids only when the THz radiation was tuned away from strongly-absorbing transitions; and (2) Ultrasound produced notable hot spots whenever there was poor interfacial adhesion between components of a composite material. Home-made explosives would most likely have worse interfacial adhesion than explosives made in a factory.

Literature cited

1. C. M. Berg, A. Lagutchev, and D. D. Dlott, Probing of molecular adsorbates on Au surfaces with large-amplitude temperature jumps, *J. Appl. Phys.* **113**, 183509 (2013).
2. A. Barua, S. Kim, Y. Horie, and M. Zhou, Ignition criterion for heterogeneous energetic materials based on hotspot size-temperature threshold, *J. Appl. Phys.* **113**, 064906 (2013).
3. B. C. Pein and D. D. Dlott, Modifying Vibrational Energy Flow in Aromatic Molecules: Effects of Ortho Substitution, *J. Phys. Chem.* **118**, 965-973 (2014).
4. B. C. Pein, Y. Sun, and D. D. Dlott, Unidirectional vibrational energy flow in nitrobenzene, *J. Phys. Chem. A* **117**, 6066-6072 (2013).
5. C. M. Tarver, S. K. Chidester, and A. L. Nichols III, Critical conditions for impact- and shock-induced hot spots in solid explosives, *J. Phys. Chem.* **100**, 5794-5799 (1996).
6. Y. Sun, B. C. Pein, and D. D. Dlott, Three-dimensional spectroscopy of vibrational energy in liquids: nitromethane and acetonitrile, *J. Phys. Chem. B* **117**, 10898-10904 (2013).
7. J. A. Carter, Z. Wang, and D. D. Dlott, Ultrafast nonlinear coherent vibrational sum-frequency spectroscopy methods to study thermal conductance of molecules at interfaces, *Acc. Chem. Res.* **42**, 1343-1351 (2009).
8. J. A. Carter, Z. Wang, H. Fujiwara, and D. D. Dlott, Ultrafast excitation of molecular adsorbates on flash-heated gold surfaces, *J. Phys. Chem. A* **113**, 12105-12114 (2009).
9. C. M. Berg, K. E. Brown, R. W. Conner, Y. Fu, H. Fujiwara, A. Lagutchev, W. L. Shaw, X. Zheng, and D. D. Dlott, Experiments probing fundamental mechanisms of energetic material initiation and ignition, *Mater. Res. Soc. Symp. Proc.* **1405**, Y06-01 (2012).
10. C. M. Berg, A. Lagutchev, and D. D. Dlott, Probing of molecular adsorbates on Au surfaces with large-amplitude temperature jumps, *J. Appl. Phys.* **113**, 183509 (2013).
11. C. M. Berg, A. Lagutchev, Y. Fu, and D. D. Dlott, Nitro stretch probing of a single molecular layer to monitor shock compression with picosecond time resolution, *AIP Confer. Proc.* **1426**, 1573-1596 (2012).
12. C. M. Berg, Y. Sun, and D. D. Dlott, Temperature-dependent dynamic response to flash heating of molecular monolayers on metal surfaces: Vibrational energy exchange, *J. Phys. Chem. B* **118**, 7770-7776 (2013).
13. A. Lagutchev, S. A. Hambir, and D. D. Dlott, Nonresonant background suppression in broadband vibrational sum-frequency generation spectroscopy, *J. Phys. Chem. C* **111**, 13645-13647 (2007).

14. A. Lagutchev, A. Lozano, P. Mukherjee, S. A. Hambir, and D. Dlott, Compact broadband vibrational sum-frequency generation spectrometer with nonresonant suppression, *Spectrochim. Acta. A* **75**, 1289–1296 (2010).
15. M.-W. Chen, S. You, K. S. Suslick, and D. D. Dlott, Hot spots in energetic materials generated by infrared and ultrasound, detected by thermal imaging microscopy, *Rev. Sci. Instrum.* **85**, 023705 (2014).
16. M.-W. Chen, S. You, K. S. Suslick, and D. D. Dlott, Hot spot generation in energetic materials created by long-wavelength infrared radiation, *Appl. Phys. Lett.* **104**, 061907 (2014).
17. S. You, M.-W. Chen, D. D. Dlott, and K. S. Suslick, Ultrasonic hammer produces hot spots in solids, *Nature Commun.* **6**, 6581 (2014).
18. B. C. Pein and D. D. Dlott, “Vibrational energy and molecular thermometers in liquids: Ultrafast IR-Raman spectroscopy,” in *Ultrafast Infrared Vibrational Spectroscopy*, edited by M. D. Fayer (CRC Press Taylor & Francis Group, Boca Raton, FL, 2013), pp. 269-304.
19. C. M. Berg and D. D. Dlott, “Vibrational sum-frequency generation spectroscopy of interfacial dynamics,” in *Vibrational Spectroscopy of Electrically-Charged Interfaces*, edited by A. Wiecekowsky, C. Korzeniewski, and B. Braunschweig (Wiley, Hoboken N. J., 2013), pp. 85-119.
20. Y. Fu, E. A. Friedman, K. E. Brown, and D. D. Dlott, Vibrational spectroscopy of nitroaromatic self-assembled monolayers under extreme conditions, *Chem. Phys. Lett.* **501**, 369-374 (2011).
21. K. E. Brown and D. D. Dlott, High pressure Raman spectroscopy of molecular monolayers adsorbed on a metal surface, *J. Phys. Chem. C* **113**, 5751-5757 (2009).
22. Z. Wang, J. A. Carter, A. Lagutchev, Y. K. Koh, N.-H. Seong, D. G. Cahill, and D. D. Dlott, Ultrafast flash thermal conductance of molecular chains, *Science* **317**, 787-790 (2007).

Quantitative metrics

A. Published papers

1. C. M. Berg, K. E. Brown, R. W. Conner, Y. Fu, H. Fujiwara, A. Lagutchev, W. L. Shaw, X. Zheng, and D. D. Dlott, Experiments probing fundamental mechanisms of energetic material initiation and ignition, *Mater. Res. Soc. Symp. Proc.* **1405**, Y06-01 (2012).
2. H. Fujiwara, K. E. Brown, and D. D. Dlott, A thin-film Hugoniot measurement using a laser-driven flyer plate, *AIP Confer. Proc.* **1426**, 382-385 (2012).
3. C. M. Berg, A. Lagutchev, Y. Fu, and D. D. Dlott, Nitro stretch probing of a single molecular layer to monitor shock compression with picosecond time resolution, *AIP Confer. Proc.* **1426**, 1573-1596 (2012).
4. K. E. Brown, R. Conner, Y. Fu, H. Fujiwara, and D. D. Dlott, Microscopic states of shocked polymers, *AIP Confer. Proc.* **1426**, 1593-1596 (2012).
5. C. M. Berg, A. Lagutchev, and D. D. Dlott, Probing of molecular adsorbates on Au surfaces with large-amplitude temperature jumps, *J. Appl. Phys.* **113**, 183509 (2013).
6. C. M. Berg, Y. Sun, and D. D. Dlott, Temperature-dependent dynamic response to flash heating of molecular monolayers on metal surfaces: Vibrational energy exchange, *J. Phys. Chem. B* **118**, 7770-7776 (2013).
7. B. C. Pein, Y. Sun, and D. D. Dlott, Unidirectional vibrational energy flow in nitrobenzene, *J. Phys. Chem. A* **117**, 6066-6072 (2013).
8. B. C. Pein, Y. Sun, and D. D. Dlott, Controlling vibrational energy flow in liquid alkylbenzenes, *J. Phys. Chem. B* **117**, 10898-10904 (2013).
9. Y. Sun, B. C. Pein, and D. D. Dlott, Three-dimensional spectroscopy of vibrational energy in liquids: nitromethane and acetonitrile, *J. Phys. Chem. B* **117**, 10898-10904 (2013).
10. M.-W. Chen, S. You, K. S. Suslick, and D. D. Dlott, Hot spots in energetic materials generated by infrared and ultrasound, detected by thermal imaging microscopy, *Rev. Sci. Instrum.* **85**, 023705 (2014).
11. M.-W. Chen, S. You, K. S. Suslick, and D. D. Dlott, Hot spot generation in energetic materials created by long-wavelength infrared radiation, *Appl. Phys. Lett.* **104**, 061907 (2014).
12. D. Curtis and D. D. Dlott, Dynamics of shocks in laser-launched flyer plates probed by photon Doppler velocimetry, *J. Phys.: Conf. Ser.* **500**, 192002 (2014).
13. C. Pein and D. D. Dlott, Modifying Vibrational Energy Flow in Aromatic Molecules: Effects of Ortho Substitution, *J. Phys. Chem.* **118**, 965-973 (2014).
14. S. You, M.-W. Chen, D. D. Dlott, and K. S. Suslick, Ultrasonic hammer produces hot spots in solids, *Nature Commun.* **6**, 6581 (2014).

B. Presentations

Dana Dlott

1. (invited) "Molecular transformations and energy transfer at interfaces", USC-DOE conference on "Materials for Energy Applications - Experiment, Modeling and Simulations", Mar. 2011, Los Angeles, CA.

2. (*invited*) Studium Conference on in situ molecular spectroscopic technique and application, Orleans, France, June 2011, "In situ probing by time-resolved vibrational spectroscopy: shocked materials and energy storage media"
3. (*invited*) American Chemical Society National Meeting, Denver, CO Aug. 2011, "Interfaces under extreme conditions"
4. (*invited*), Federation of analytical chemistry and spectroscopy (FACSS) national meeting, Reno, NV, Oct. 2011, "Three dimensional vibrational spectroscopy of molecular energy".
5. (*invited*) "Interfaces under extreme conditions", Oct. 2011, Rice University Department of Chemistry
6. (*invited*) "Ultrafast shock compression spectroscopy", Oct. 2011, Carnegie Defense Alliance Annual Review, Argonne National Laboratory.
7. (*invited*) Materials Research Society National Meeting, Boston, MA Nov. 2011, "Experiments Probing Fundamental Mechanisms of Energetic Material Initiation and Ignition"
8. (*invited*) "Interfaces under extreme conditions", National Chiao Tung University Department of Chemistry, Hsinchu, Republic of China, Feb. 2012.
9. (*invited*) "Spontaneous energy concentration in energetic molecules, interfaces and composites: response to ultrasound and THz radiation", Office of Naval Research Program Review, Basic Research - Sciences Addressing Asymmetric Explosive Threats, Arlington, VA May 21, 2012.
10. (*invited*) "Experiments probing initiation and ignition of energetic materials", International Center for Applied Computational Mechanics (ICACM) symposium New York, NY June 11-13 2012.
11. (*invited*) "Shock physics for dummies!", Gordon Conference on Energetic Materials, W. Dover, VT, June 2012.
12. (*invited*) "Molecular dynamics of explosives" Department of Chemistry, Colorado State University, Ft. Collins, CO, Oct. 2012.
13. (*invited*) "Laser-driven flyer plates for shock compression spectroscopy", International Symposium on Pulsed Power Applications, Kumamoto University, Kumamoto, Japan, Mar. 2013
14. (*invited*) "Ultrafast spectroscopy of molecules at metal surfaces", University of Florida, Department of Chemical Engineering, Gainesville, FL, Mar. 2013.
15. (*invited*) "Laser-driven flyer plates for shock wave spectroscopy", Los Alamos National Laboratory, May 2013.
16. "Laser-driven flyer plates for shock wave spectroscopy", APS SCCM Meeting, Seattle, WA, July 2013
17. (*invited*) "Ultrafast vibrational spectroscopy of energy flow in molecules", CECAM Workshop on Nanophononics, Bremen, Germany, Aug. 2013
18. (*invited*) "Vibrational energy transfer on surfaces and in liquids". ACS National Meeting, Indianapolis, IN Sept. 2013.
19. (*invited*) "Molecular dynamics of explosives," Rochester Institute of Technology, Department of Chemistry and Materials Science, Rochester, NY, Oct. 2013
20. (*invited*) "Ultrafast vibrational spectroscopy of shocked energetic materials". AFOSR Dynamic Materials and Interactions Portfolio Review, Arlington, VA, Oct. 2013.
21. (*invited*) "SFG studies of buried electrochemical interfaces," ACS National Meeting, Dallas, TX, Mar. 2014.

22. "Probing dynamic material interfaces using nonlinear coherent vibrational spectroscopy", AFOSR Dynamic Interfaces Workshop, Arlington, VA, Mar. 2014.
23. "Probing shocked microstructured energetic materials", AFOSR Dynamic Interfaces Workshop, Arlington, VA, Mar. 2014.
24. *(invited)* "Vibrational energy transfer on surfaces and in liquids, MIT Modern Optics and Spectroscopy Seminar, Apr. 2014.
25. *(invited)* "Shock wave energy dissipation, ONR SWED MURI review, Arlington, VA, June 2014.
26. *(invited)* "Shock wave energy dissipation, Office of Secretary of Defense 2014 MURI Program Review, Arlington, VA, July 2014.
27. *(invited)* "Ultrafast diagnostics for high-speed impacts with particulate composites", DTRA program review, Springfield, VA, July 2014
28. *(invited)* "Vibrational spectroscopy in extreme environments: Watching stressed-out molecules", Gordon Conference on Vibrational Spectroscopy, Biddeford, ME, Aug. 2014.
29. *(invited)* "Time-resolved spectroscopy of shocked energetic materials", Triservice Energetic Materials Basic Science Review, Arlington, VA, Sept. 2014.
30. *(invited)* "Molecular dynamics of explosions", Departments of Chemistry and Physics, Indiana State University, Terre Haute, IN, Sept. 2014.
31. *(invited)* "Spectroscopy of materials under extreme conditions", Department of Chemistry, Johns Hopkins University, Baltimore, MD, Oct. 2014.
32. *(invited named lectureship)* "Materials chemistry under extreme conditions", Bryce Crawford Lecture, Department of Chemistry, University of Minnesota, Minneapolis, MN, Apr. 2015.
33. *(invited)* "Time-resolved spectroscopy of shock-compressed materials", AFOSR Molecular Dynamics and Theoretical Chemistry contractors' meeting, Albuquerque, NM, May 2015
34. *(plenary)*, "Shock compression dynamics under a microscope), APS Biennial Conference on Shock Compression of Condensed Matter, Tampa, FL, June 2015.
35. *(invited)*, "Real-time shock compression in microstructured materials", AFOSR Dynamic Material Interfaces Program Review, Pensacola, FL, Aug. 2015.
36. *(invited)*, "Shock compression spectroscopy under a microscope", Carnegie Defense Alliance NNSA program review, Argonne National Lab, Dec. 2015.

Kenneth Suslick

- (Invited)* International Congress on Acoustics (ICA 2013), Montreal, June 2013.
- (Invited)* Wilsmore Lecturer, "The Chemical & Physical Effects of Ultrasound", U. Melbourne, July 2013.
- (Invited)* "The Chemical & Physical Effects of Ultrasound", Department of Chemistry Texas Tech, Feb., 2014.
- (Invited)*, "The Chemical & Physical Effects of Ultrasound", Pure Chemistry Award Symposium, ACS National Meeting, Dallas, TX Apr. 2014.
- Summary Lecturer, "The Chemical & Physical Effects of Ultrasound", Faraday Discussion Symposium on Mechanochemistry, Montreal, May 2014.
- (Plenary)* "The Chemical & Physical Effects of Ultrasound", 14th European Sonochemistry Society Meeting, Avignon, June, 2014.

(Plenary) "The Chemical & Physical Effects of Ultrasound", Ultrasonics 2014, Lisbon, Sept., 2014.
(Invited) "Nanoscale chemistry with ultrasound", Arizona State University, Tempe, Nov. 2015.
(Invited) "Hot spots in solids", Bradley University, Peoria, Oct. 2015.
(Invited) "Hot spots in solids", Backeland Award Symposium, Rutgers University, New Jersey, Dec. 2015.
(Invited), "Nanoscale chemistry with ultrasound", Symp. on Application of Ultrasound to Nanoscience, Pacificchem 2015, Honolulu, Dec. 2015.
Invited Speaker, "Hot spots in solids", Symp. on Chemical Reactions by Innovative Technologies, Pacificchem 2015, Honolulu, Dec. 2015.

Mingwei Chen

"Shock Compression Induced Hot Spots in Energetic Material Detected by Thermal Imaging Microscopy", 69th International Symposium on Molecular Spectroscopy, Urbana, IL, June, 2014.
"Infrared and Ultrasound Induced Hot Spots in Energetic Materials: A Microscopic Thermal Imaging Study", 248th ACS Meeting, San Francisco, CA, Aug. 2014.

Sizhu You

Ultrasonic Hot Spots in Polymer Composites. ACS Fall National Meeting, 2014. (poster)
Ultrasonic Hot Spots in Solids. Department of Chemistry, UIUC, 2014. (oral)
Ultrasonic Hot Spots in Polymer Composites. MRS Spring Meeting, 2014. (oral)

C. People working on the project

Dana D. Dlott PI
Kenneth S. Suslick, co-PI
Mingwei Chen, postdoc, now at Sandia Livermore
Alexander Curtis, postdoc
Alexandr Banishev, postdoc
Zhiwei Men, visiting professor from Harbin Institute of Technology
Sizhu You, graduate student, now with Saint-Gobain North America
Christopher M. Berg, graduate student, now with Defense Nuclear Facilities Safety Board
Brandt C. Pein, graduate student, now postdoc at MIT
Yuxiao Sun, graduate student